Antimicrobial Hydantoin-Containing Polyesters[a]

Licheng Tan, Samarendra Maji, Claudia Mattheis, Mengyao Zheng, Yiwang Chen,* E. Caballero-Díaz, Pilar Rivera Gil, Wolfgang J. Parak, Andreas Greiner, Seema Agarwal*

A new *N*-hydantoin-containing biocompatible and enzymatically degradable polyester with antibacterial properties is presented. Different polyesters of dimethyl succinate, 1,4-butanediol, and 3-[*N,N*-di(*β*-hydroxyethyl)aminoethyl]-5,5-dimethylhydantoin in varying molar ratios are prepared via two-step melt polycondensation. The antibacterially active *N*-halamine form is obtained by subsequent chlorination of the polyesters with sodium hypochlorite. Chemical structures, thermal properties, and spherulitic morphologies of the copolymers are studied adopting FT-IR, NMR, TGA, DSC, WAXD, and POM. The polyesters exhibit antibacterial activity against *Escherichia coli*. The adopted synthetic approach can be transferred to other polyesters in a straightforward manner.

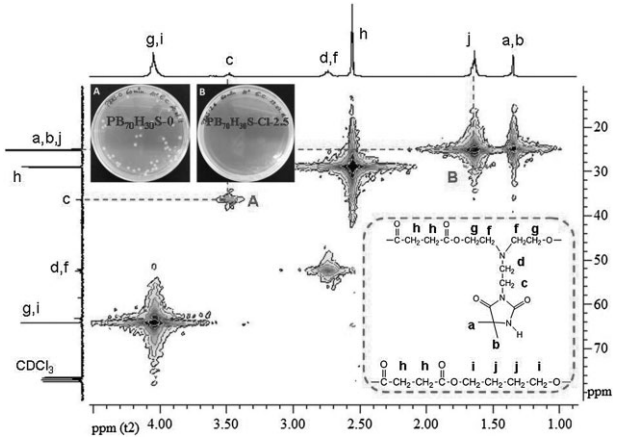

L. Tan, S. Maji, C. Mattheis, A. Greiner, S. Agarwal
Department of Chemistry and WZMW, Philipps-Universität Marburg, Hans-Meerwein-Str., 35032 Marburg, Germany
E-mail: agarwal@staff.uni-marburg.de
L. Tan, Y. Chen
Department of Chemistry, Nanchang University, 999 Xuefu Avenue, Nanchang 330031, China
E-mail: ywchen@ncu.edu.cn
M. Zheng
Department of Pharmaceutics and Biopharmacy, Philipps-Universität Marburg, 35037 Marburg, Germany
E. Caballero-Díaz, P. R. Gil, W. J. Parak
Department of Physics and WZMW, Philipps-Universität Marburg, Renthof 7, 35037 Marburg, Germany

[a] **Supporting Information** for this article is available from the Wiley Online Library or from the author.

1. Introduction

Recently, materials that controlling microbial colonization on solid surfaces are of great concern in a wide field of industrial, environmental, institutional, and hygienic applications.[1] In order to obtain such materials, the introduction of biocides is the most common approach. These biocides for example can consist of quaternary ammonium salts,[2–5] phosphonium salts,[6,7] metal ions and oxides,[8,9] and cyclic *N*-halamine compounds.[10–12] The latter are particularly in the focus of attention because they exhibit a long-term stability, comprise a biocidal effect against a broad range of micro-organisms, and are regenerable upon exposure to household bleach. A lot of efforts were made to synthesize various *N*-halamine based antibacterial materials of both low and high molecular

weights. In one of the approaches, either *N*-halamine containing polymers or low-molecular-weight *N*-halamine derivatives were added as additives to impregnate the respective polymers in order to obtain antibacterial materials[13–15] *N*-halamine precursor structures were also incorporated into poly(propylene)[16] and low density polyethylene[17] by a reactive extrusion process. The other recent approaches involve functionalization by chemical reactions (e.g., a direct functional group transformation, homo- and/or copolymerization, grafting, etc.)[18–22] to introduce *N*-halamine structures into the desired matrix polymers. Worley and coworkers have done extensive work on antibacterial materials based on *N*-halamine.[23] They have provided *N*-halamine based new materials and many novel concepts of attaching *N*-halamine moieties to various polymers either by copolymerization or by polymer analogous reactions and layer-by-layer process. Some of the representative literature of Worley and coworkers on the topic is highlighted as ref.[23] In one of the studies, Worley and coworkers synthesized an *N*-halamine containing monomer based on a siloxane structure, which was covalently attached to the surface of cotton fibers.[21] The chlorinated species showed a biocidal activity against *Staphylococcus aureus* and *Escherichia coli* (*E. coli*). Aromatic polyamide membranes were functionalized by grafting with a hydantoin derivative to improve their resistancy against chlorine and their antibiofouling properties.[24] *N*-halamine functionalized polyurethane coatings were also made by reaction of diol functionalized with hydantoin and acrylic polyols and isocyanates using a step growth polyaddition reaction.[25] *N*-halmine based various vinyl monomers are also known. Sun and Sun[20] for example synthesized a monomer comprising 3-(4'-vinylbenzyl)-5,5-dimethylhydantoin (VBDMH) as the active functionality. Subsequently it was copolymerized with various comonomers like vinyl acetate, acrylonitrile, and methyl methacrylate; the copolymers showed very good antibacterial properties after chlorination.

Although the representative highlighted literature shows significant contributions regarding *N*-halamine polymers but hydantoin moieties have never been incorporated directly into polyester by high temperature melt polycondensation reaction yet, to the best of our knowledge. In this work, 3-[*N,N*-di(β-hydroxyethyl)aminoethyl]-5,5-dimethylhydantoin was adopted as diol comonomer and was combined with both 1,4-butanediol (BDO) and dimethyl succinate (DMS) to synthesize copolyesters. The antibacterial active *N*-halamine form was obtained by a subsequent chlorination of the polyesters with sodium hypochlorite. Chemical structure, thermal properties and spherulitic structure of the synthesized copolymers containing hydantoin moieties were investigated via Fourier-transform infrared (FT-IR) and NMR spectroscopy, thermogravimetric analysis (TGA), differential scanning calorimetry (DSC), wide-angle X-ray diffraction (WAXD), and polarized optical microscopy (POM). To elucidate the biocompatibility/cytotoxicity of the materials, 3-(4,5-dimethylthiazol-2-yl)-2,5-diphenyltetrazolium bromide (MTT) tests with L929 cells were conducted, and the antibacterial activity was examined against *E. coli* as Gram-negative test organism.

2. Experimental Section

2.1. Materials

5,5-Dimethylhydantoin (DMH) and DMS were purchased from Alfa Aesar Co., Ltd. 1-bromo-2-chloroethane and 18-crown-6 ether were from Sigma-Aldrich. Diethanolamine (DEA, Sigma-Aldrich, ≥98%) and BDO were distilled under vacuum and stored under argon. Titanium (IV) butoxide [$Ti(OBu)_4$] was purchased from Acros Organics and the lipase of *Pseudomonas cepacia* was acquired from Sigma-Aldrich. *N,N*-Dimethylformamide (DMF) was distilled from calcium hydride under reduced pressure. All other chemicals and solvents of analytical grade were used as received without further purification.

2.2. Characterization

FT-IR spectra were recorded on a Digilab Excalibur Series system using a Pike Miracle attenuated total reflection (ATR) unit. The samples were measured in powdered state without further preparation. Win-IR Pro 3.3 (Digilab) was used for data recording and interpretation. ^{1}H (300 MHz) and ^{13}C (75 MHz) NMR spectra were recorded on a Bruker DRX-300 spectrometer using deuterated chloroform ($CDCl_3$) as solvent. Chemical shifts (δ) are reported relative to tetramethylsilane (TMS) as internal reference. For calibration the residual signal of the deuterated $CDCl_3$ was set to $\delta = 7.26$ (^{1}H NMR) and $\delta = 77.0$ (^{13}C NMR). ^{1}H-^{13}C heteronuclear multiple quantum correlation (HMQC) experiments were performed on a Bruker DRX-500 spectrometer, with a 5 mm multinuclear gradient probe and using gs-HMQC pulse sequences. Molecular weights of the polymers were determined by gel permeation chromatography (GPC) using a Knauer system equipped with one column, PSS-SDV (linear XL, 5 μm, 8.0 × 300 mm^2), a differential refractive-index detector, $CHCl_3$ as eluent at a flow rate of 0.5 mL · min^{-1}. All measurements were done against the standard calibration with poly(methyl methacrylate) (PMMA). Toluene was used as internal standard. TGA was performed on a TGA/SDTA 851e (Mettler Toledo) at a heating rate of 10 °C · min^{-1} under nitrogen with a sample size of 8–10 mg. DSC measurements of polymers were carried out on a DSC 821e unit (Mettler Toledo) under a nitrogen flow at a rate 80 mL · min^{-1}. About 7 mg sample were encapsulated in the DSC aluminum pan, heated quickly to 150 °C and held for 5 min to erase the thermal history. Then, the samples were cooled to −50 °C and subsequently heated to 150 °C at a rate of 5 °C · min^{-1}. The corresponding glass transition temperature (T_g), melting temperature (T_m), crystallization temperature (T_c), melting enthalpy (ΔH_m), and crystallization enthalpy (ΔH_c) were recorded, respectively. X-ray diffraction patterns of the samples were recorded with a Siemens goniometer D5000 using

Macromol. Biosci. 2012, DOI: 10.1002/mabi.201100520

Cu-K_α radiation of $\lambda = 1.54$ Å. The spherulitic morphology of the polymers was analyzed by a Leica DMRX POM fitted with a Leica DC200 camera at a magnification of 1:100.

2.3. Synthesis of 3-(2′-Chloroethyl)-5,5-dimethylhydantoin

5,5-Dimethylhydantoin (DMH, 96.1 g, 0.75 mol), was dissolved in a solution of 42.1 g (0.75 mol) KOH in 500 mL ethanol. This solution was mixed with 215.1 g (1.5 mol) 1-bromo-2-chloroethane in one portion. The resulting solution was refluxed at 80 °C for 8 h. Evaporation of the reaction mixture resulted in a white solid which was shaken with ethyl acetate and water in a separatory funnel. The organic layer was separated, washed (10% aqueous $NaHCO_3$), dried (Na_2SO_4), and evaporated to isolate the product. Recrystallization from toluene/2-propanol (1:9 v/v) resulted in white crystals with a yield of 92%. This compound was identified as 3-(2′-chloroethyl)-5,5-dimethylhydantoin. ^{1}H NMR ($CDCl_3$, 300 MHz, δ): 1.46 (6H, CH_3), 3.75 (2H, CH_2), 3.84 (2H, CH_2), 6.61 (1H, N−H).

2.4. Synthesis of 3-[*N,N*-di(β-hydroxyethyl)aminoethyl]-5,5-dimethylhydantoin

3-(2′-Chloroethyl)-5,5-dimethylhydantoin 38.0 g (0.20 mol), potassium iodide (KI) 49.8 g (0.30 mol), DEA 31.5 g (0.30 mol), and 18-crown-6-ether 10.6 g (0.04 mol) were dissolved in 200 mL of freshly distilled *N,N*-dimethylformamide (DMF). The resulting solution was heated to 100 °C for 20 h. After removing DMF at reduced pressure, the residue was treated with saturated aqueous $NaHCO_3$ solution. This solution was extracted with ethyl acetate twice, dried over Na_2SO_4, filtered, and evaporated to result in an oily residue. By column chromatography on silica gel with ethyl acetate/hexane (1:1 v/v) and dichloromethane/methanol (10:1 v/v) as eluent, 3-[*N,N*-di(β-hydroxyethyl)aminoethyl]-5,5-dimethylhydantoin was obtained in a yield of 25–30%. ^{1}H NMR ($CDCl_3$, 300 MHz, δ): 1.46 (6H, CH_3), 2.67 (4H, CH_2), 2.75 (2H, CH_2), 3.53 (4H, CH_2), 3.58 (2H, CH_2), 6.58 (1H, N−H).

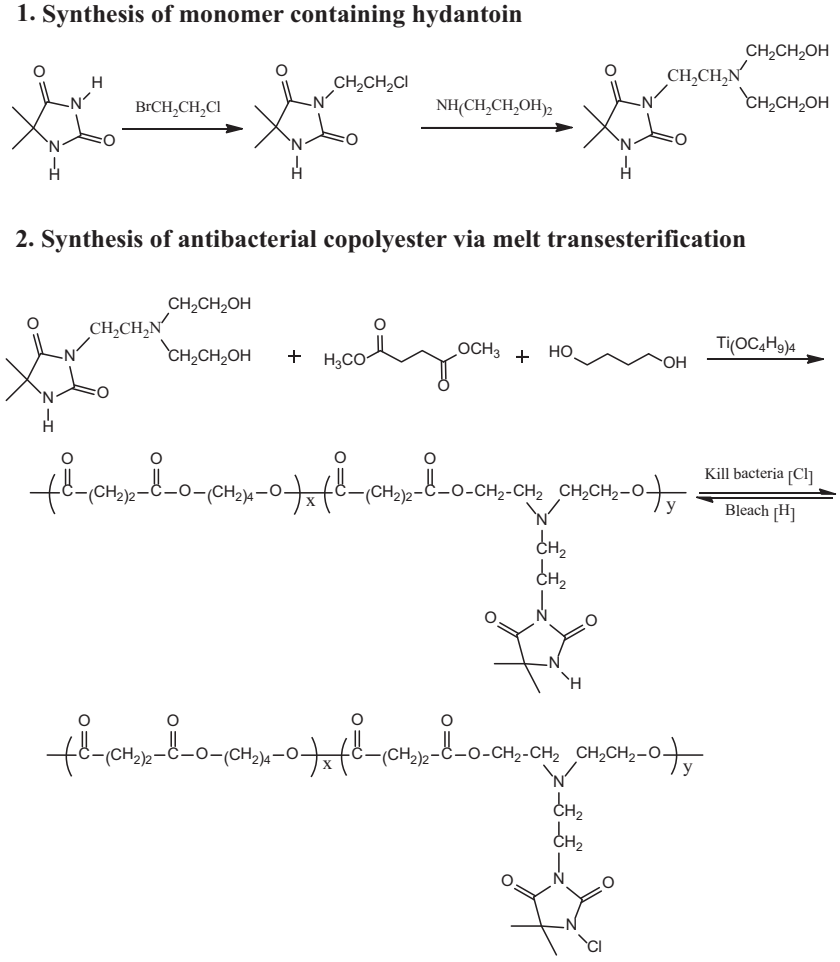

Scheme 1. Synthesis of monomers and copolyesters containing hydantoin and the chlorination process to obtain the antibacterial halamine derivatives.

2.5. Synthesis of Copolyesters

Poly[(butylene succinate)-*co*-(hydroxyethylaminoethyldimethylhydantoin succinate)] (PBHS) copolyesters were synthesized via a two-step melt polycondensation process consisting of esterification and polycondensation in the presence of DMS, BDO, and the hydantion-containing monomer, as shown in Scheme 1. Molar ratios of total diol to DMS of 1.2 to 1, and 0.1 mol% $Ti(OBu)_4$ regarding the total chemicals were used. After charging into a flask, the mixture was heated to 170 °C and reacted for 2 h under nitrogen with vigorous stirring. After a certain amount of methanol had been collected by distillation, the esterification was considered as completed and stopped. The pressure was gradually reduced and the reaction carried on for another 5 h to obtain copolyesters of higher molecular weights. After completion of the polycondensation, the mixture was cooled down to room temperature, dissolved in 20 mL chloroform and precipitated from 500 mL pentane. The precipitate was collected and dried under vacuum at 40 °C for 24 h.

2.6. Chlorination of the $PB_{70}H_{30}S$ Copolyester

Polymer films were cast from chloroform solution. The films (thickness about 0.06 mm) were cut into small pieces (10 × 10 mm^2), and treated with 20 mL of a 6.0% sodium hypochlorite solution. The chlorination was performed by vigorous stirring for 1.5–2.5 h at 45 °C. Subsequently the films were thoroughly washed with distilled water, dried at room temperature for 20 h, and then under reduced pressure at 40 °C for 2 h to remove free chlorine.

The chlorine content of the $PB_{70}H_{30}S$ copolyester was analyzed by using an iodometric method. 0.1 ± 0.001 g of each sample were immersed in 25 mL of a sulfuric acid solution for 10 min. 1 g of KI and a few drops of a 1% starch solution were added as indictors. The mixture was titrated with a solution of $0.01\,mol \cdot L^{-1}$ sodium thiosulfate immediately. The amount of active chlorine was calculated according to

$$Cl\% = \frac{35.45}{2} \times \frac{V_{Na_2S_2O_3} \times C_{Na_2S_2O_3}}{W_S} \times 100\% \quad (1)$$

where Cl% is the amount of oxidative chlorine on the samples in weight percent, $V_{Na_2S_2O_3}$ the volume of sodium thiosulfate solution consumed in the titration of the chlorinated samples in L, $C_{Na_2S_2O_3}$ the normality of the standardized sodium thiosulfate solution in $mol \cdot L^{-1}$, and W_S is the weight of the chlorinated sample in g, respectively.

2.7. Cytotoxicity Test

Cytotoxicity was determined in quadruplicate using the MTT assay. L929 cells were seeded in 96-well microtiter plates (8000 cells per well) in Dulbecco's modified Eagle medium (DMEM) low glucose supplemented with 10% fetal calf serum (Cytogen, Sinn, Germany) in humidified atmosphere with 5% CO_2 at 37 °C, 24 h prior to application of increasing concentrations of the polymer solutions. After an initial incubation of 24 h, medium was replaced with 100 μL fresh medium and 100 μL polymer suspensions in water (0.000152, 0.00046, 0.00137, 0.00412, 0.01234, 0.03703, 0.11111, 0.33333, 1 $mg \cdot mL^{-1}$ in cell culture media) were added to the cells, which were incubated for another 24 h. After the incubation period, the polymer solutions were replaced with 200 mL serum free medium containing 0.5 $mg \cdot mL^{-1}$ MTT (Sigma-Aldrich, Germany). Cells were incubated for another 4 h at 37 °C in humidified atmosphere, before the unreacted dye was removed and 200 mL dimethyl sulfoxide (DMSO) was added to dissolve the purple formazane product. After 15 min incubation with DMSO, the absorption was quantified using a plate reader (Titertek plusMS 212, ICN, Germany) at wavelengths of 570 and 690 nm. The IC_{50} values were calculated as polymer concentration which inhibits the growth of 50% cells relative to nontreated control cells.

2.8. Enzymatic Degradation

To investigate the enzymatic degradation, copolyester films before and after chlorination ($20 \times 20 \times 0.06\,mm^3$), cast from chloroform solutions, were placed in vials containing 10 mL of phosphate buffer solution (Na_2HPO_4/KH_2PO_4, pH = 7.0 at 25 °C) with 0.30 $mg \cdot mL^{-1}$ *Pseudomonas cepacia* lipase at a constant temperature of 37 °C. The buffer solution with enzyme was renewed every 3 d. At predetermined degradation time intervals, the specimens were removed from the medium, rinsed with distilled water, dried under vacuum at room temperature for 48 h, and weighed. Weight loss percentages of the copolyesters were obtained from

$$\text{Weight loss}(\%) = \frac{W_0 - W_r}{W_0} \times 100\% \quad (2)$$

where W_0 is the initial weight and W_r is the dry weight of the specimens after degradation.

2.9. Antibacterial Test

The obtain the inoculum for the antibacterial tests, a single colony *E. coli* (DSM No. 1077, K12 strain 343/113, DSZM Braunschweig), preserved on tryptic soy agar at 4 °C was transferred to tryptic soy broth (TSB, Sigma-Aldrich; dissolved in water, $c = 30\,g \cdot L^{-1}$) with an inoculation loop. The inoculated broth was incubated with shaking at 37 °C until the optical density at 578 nm had increased by 0.125, indicating a density of viable cells of 10^7–10^8 $cfu \cdot mL^{-1}$, and diluted to an approximate concentration of 10^6 $cfu \cdot mL^{-1}$ to result in the final inoculum. The exact number of colony forming units per mL in the inoculum was determined by the spread plate method. To evaluate the antibacterial properties of the copolyesters, films exhibiting a size of $\approx 5 \times 5\,mm^2$ were inoculated with 10 μL inoculum and covered with a second film each. After given time intervals (5, 15, 30, and 60 min), these "sandwiches" were vigorously washed by immersion in 10 mL of a 0.03% sodium thiosulfate solution in sterile water to remove any residues of oxidative chlorine, using a vortex mixer. A 100 μL aliquot of each solution was then serially diluted with sterile potassium buffer solution (pH = 7.4), 100 μL of each dilution were spread on nutrient agar plates. By counting of the formed colonies after incubation at 37 °C for 24 h, the number of viable cells in the solutions was determined and the reduction was calculated respective to the inoculum. Unchlorinated control samples were treated in the same manner.

3. Results and Discussion

3.1. Synthesis and Characterization of Copolyesters

By a modified procedure of the known approach, the hydantoin containing diol 3-[*N,N*-di(β-hydroxyethyl)aminoethyl]-5,5-dimethylhydantoin (H-diol) was synthesized successfully in a two-step reaction (Scheme 1).[26] Structural characterization was accomplished using NMR spectroscopic techniques and subsequently, H-diol was adopted as comonomer with BDO and DMS in the copolyester (PBHS) synthesis. "B" in the sample code represents the butylene succinate unit, and "H" stands for hydroxyethylaminoethyldimethylhydantoin succinate unit, respectively. The subscript numbers at the end of each unit indicate the molar ratio among BS and HS units in the copolyesters.

FT-IR and NMR analysis were applied to confirm the structure of the synthesized copolyesters. The FT-IR spectra of the PBHS copolyesters showed the N–H···O=C hydrogen bonded carbonyl bands around 1773 cm^{-1} and the N–H stretching bands above 3000 cm^{-1}, which were attributed to the amide carbonyl structures of the hydantoin ring, in comparison to that of PBS homopolymer. Figure 1 depicts the ^1H NMR spectra of the PBHS copolyesters compared to the corresponding homopolyesters poly(butylene succinic

Macromol. Biosci. 2012, DOI: 10.1002/mabi.201100520

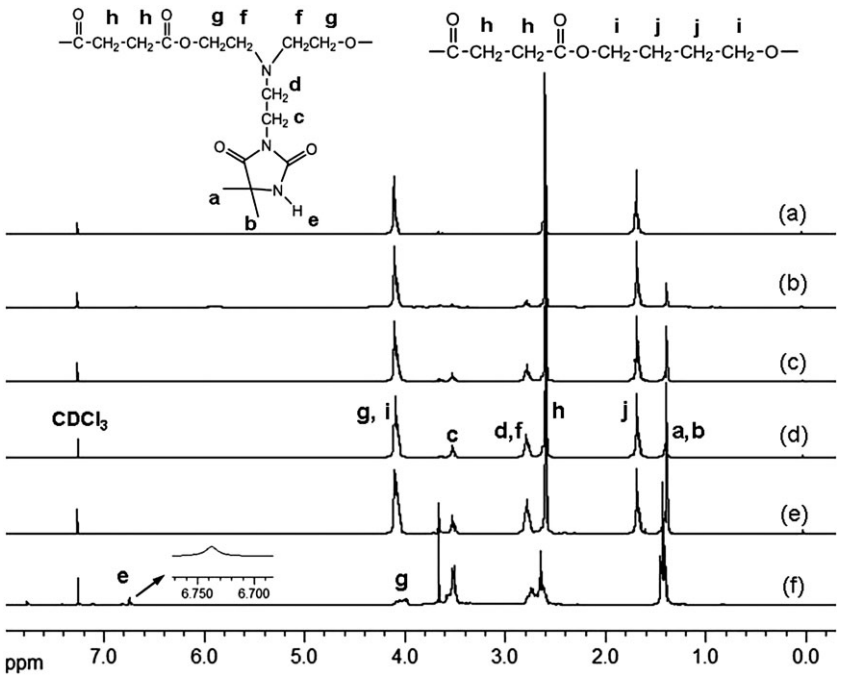

Figure 1. ^{1}H NMR spectra of PBS, PHS, and PBHS copolyesters: (a) PBS, (b) $PB_{90}H_{10}S$, (c) $PB_{80}H_{20}S$, (d) $PB_{70}H_{30}S$, (e) $PB_{60}H_{40}S$, and (f) PHS.

acid) (PBS) and poly{3-(*N,N*-di(*β*-hydroxyethyl)aminoethyl]-5,5-dimethylhydantoinsuccinic acid} (PHS). The resonances corresponding to the monomer units, i.e. B, H, and S were present in the copolyester ^{1}H NMR spectrum. The peaks at $\delta = 1.40$ (protons *a*, *b*), 3.53 (protons *c*), 2.79 (protons *d* and *f*), 4.10 (protons *g*), and 6.74 (proton *e*), could be attributed to the hydantoin (H) moiety; the signal at $\delta = 2.61$ (protons *h*) was assigned to the protons adjacent to the succinate carbonyl carbon atoms, whereas the peaks at $\delta = 4.10$ (protons *i*) and 1.69 (protons *j*) were attributed to the $-OCH_2-$ and $-CH_2-CH_2-$ protons of the butylene unit, respectively. It was observed that the relative intensity of the peaks belonging to protons *a*, *b*, *c*, *d*, and *f* increased as the amount of hydantoin (H) in the feed was more. This indicated the formation of different copolyesters with different amounts of HS units in the copolyesters.

From ^{13}C NMR spectra (not shown here), it could be seen that there was a set of four strong signals at $\delta = 25.2$ (carbons *a*, *b*), 36.4 (carbon *c*), 52.3 (carbons *d*, *f*), and 64.1 (carbon *g*) present, which was identical with the ^{13}C pattern of the hydantoin moiety, and therefore could be assigned to H units in the copolyester. The $-OCH_2-$ and $-CH_2CH_2-$ carbons of butylene exhibit overlapping resonances at $\delta = 64.1$ and 25.2 with those of the hydantoin moiety's $-CH_2$ and $-CH_3$ carbons. The peak at $\delta = 29.0$ (carbon *h*) could be assigned to carbons from the $-CH_2$ of succinate.

This peak assignment was confirmed by the ^{1}H-^{13}C HMQC NMR spectrum of $PB_{80}H_{20}S$ (Figure 2), which clearly showed two separate cross-resonances (A and B) due to the correlation of protons *c* at $\delta = 3.53$ with the carbon signal at $\delta = 36.4$ and that of protons *j* at $\delta = 1.69$ with the carbon signal at $\delta = 25.2$. Based on this, the signals at $\delta = 36.4$ and 25.2 could be assigned to the carbon atoms attached to protons *c* and *j* of the H and B units in the copolyester backbone, respectively.

The ratio of the two diols in copolyesters was calculated based on the corresponding resonance peak integrals of the protons of BDO and H-diol units at $\delta = 1.69$ and 3.53, respectively. Both diols were incorporated in the copolyesters in almost the same ratio as that of the feed. The copolymer composition was also determined using elemental analysis (N%) and was in good agreement with the values determined from ^{1}H NMR. Table 1 illustrates composition and yield of the copolyesters. Furthermore, the molecular weights of both copolyesters and the corresponding homopolyesters (PBS and PHS) were

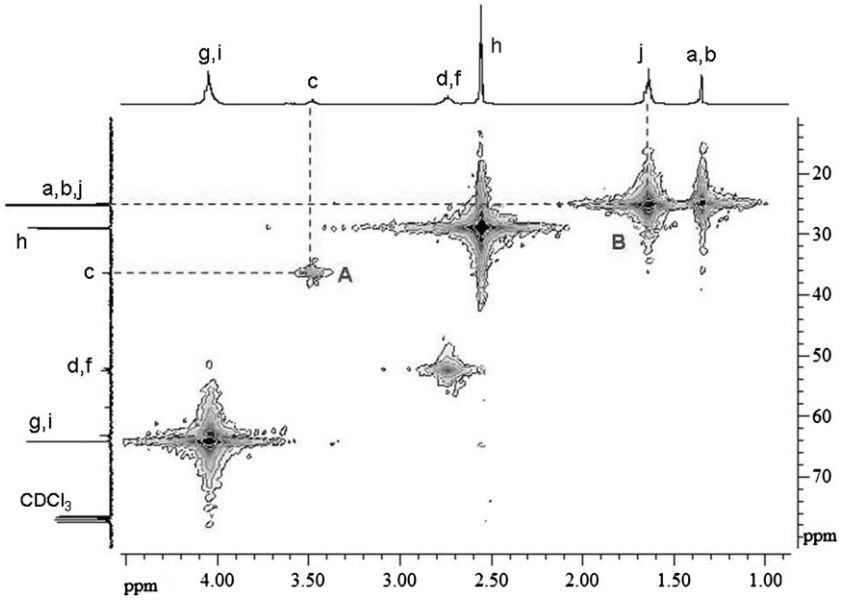

Figure 2. ^{1}H-^{13}C HMQC spectrum of the $PB_{80}H_{20}S$ copolyester.

Table 1. Melt polycondensation of DMS, BDO, and H-diol: chemical composition, yield, and molecular weights of the copolyesters.

Sample	Feed molar ratio DMS/BDO/H-diol	Molar ratio BDO/H-diol copolymer[a)]	Yield [%]	$\overline{M}_n$ [10^4 g mol^{-1}]	$\overline{M}_n/\overline{M}_w$
PBS	1.0/1.2/0	100:0 100:0	53.0	1.35	2.15
PB90H10S	1.0/1.08/0.12	90:10 89:11	54.4	1.60	2.32
PB80H20S	1.0/0.96/0.24	80:20 74:26	55.7	0.91	2.16
PB70H30S	1.0/0.84/0.36	70:30 69:31	62.3	0.93	2.20
PB60H40S	1.0/0.72/0.48	60:40 58:42	63.8	0.63	2.68
PHS	1.0/0/1.2	0:100 0:100	49.3	–	–

[a)]Molar ratio BDO/H-diol in resulting copolymers was calculated from ^{1}H NMR; these values agreed well with that from elemental analysis: $PB_{90}H_{10}S$ 2.29/2.45, $PB_{80}H_{20}S$ 4.60/3.42, $PB_{70}H_{30}S$ 5.67/5.83, $PB_{60}H_{40}S$ 7.12/7.37, PHS 11.51/13.51 (values indicate theoretical N content based on NMR data/experimental N content, both in %).

determined by GPC (Figure 3), the results are listed in Table 1. In all cases, an unimodal GPC chromatogram was obtained; the number-averaged molecular weight ($\overline{M}_n$) of the copolymers ranged from 6300 to 16 000 g · mol^{-1}, while the polydispersity was in a range of 2.68–2.16. In general, the presence of H-diol as comonomer resulted in lower molecular weights.

The polyesters were soluble in organic solvents like chloroform and tetrahydrofuran (THF) and were film forming. The films were brittle as polyesters were of low to moderate molecular weights and therefore no attempt was made to determine the mechanical properties. We carried out the literature procedure of chlorination of H units (conversion of *N*-hydantoin to *N*-halamine) by casting copolymer films, which were treated with 6% sodium hypochlorite solution at 40 °C for 2 h.[22] After chlorination, such a transformation of hydantoin to *N*-halamine structures could be observed via FT-IR and NMR spectroscopy. It was found that the band at 1733 cm^{-1} in FT-IR, which corresponded to the amide structure of the hydantoin ring, disappeared after chlorination; this indicated that a disruption of the N–H··· O=C hydrogen bonding took place upon conversion of N–H to N–Cl and confirmed the transformation of hydantoin to *N*-halamine. The disappearance of amide-hydrogen signal around $\delta = 6.74$ in ^{1}H NMR after chlorination also indicated the transformation of N–H group of the hydantoin amide into N–Cl. The active chlorine content of $PB_{70}H_{30}S$ copolyester ranged from 1.95 to 3.01%, as shown in Table 2. A significant improvement in the chlorine content (Cl%) was observed with increasing length of the bleach treatment. These chlorinated samples were further tested for antibacterial property.

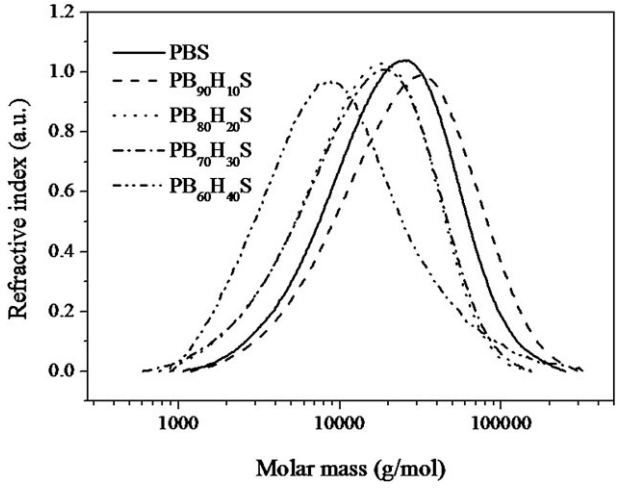

Figure 3. GPC profiles of PBS and the PBHS copolyesters.

3.2. Thermal and Crystallization Properties of Copolyesters

Thermal stability of the copolyesters was evaluated by TGA measurements conducted in nitrogen atmosphere from 25 to 800 °C. The corresponding decomposition temperatures (T_d), measured at 5% weight loss of all copolyesters, are summarized in Table 3. All copolyesters showed a high thermal stability with T_d values above 200 °C (Figure S1 Supporting Information). Except that the T_d of homopolyester PHS decreased markedly, the T_d of the rest PBHS copolyesters increased slightly compared to pure PBS, revealing that incorporating HS units slightly improved the thermal stability of the PBHS copolyesters. Crystallization and melting behavior of the copolyesters were investigated by DSC; heating and cooling curves are shown in Supporting Information (Figure S2). Table 3 provides a summary of the DSC results from first cooling and second heating scan, revealing the glass transition temperature (T_g), melting temperature (T_m), crystallization temperature (T_c), melting enthalpy (ΔH_m), as well as the crystallization enthalpy (ΔH_c). It was noticed that all copolyesters comprise only one

Table 2. Antibacterial activities of $PB_{70}H_{30}S$ copolyester before and after chlorination against *E. coli* (10^6 cfu · mL^{-1}).

Sample	Chlorination time [h]	Chlorine content [%]	Contact time [min]	Reduction [%]	Log reduction [%]
$PB_{70}H_{30}S$-0	0	0	5	2.10	0.24
			15	65.28	0.45
			30	56.36	0.36
			60	99.18	2.09
$PB_{70}H_{30}S$-Cl-1.5	1.5	1.95	5	27.10	0.95
			15	88.68	0.95
			30	99.04	2.02
			60	98.44	1.81
$PB_{70}H_{30}S$-Cl-2.5	2.5	3.01	5	74.20	0.59
			15	54.86	0.35
			30	93.75	1.20
			60	100	5.00

glass transition temperature, resulting from the formation of a homogeneous phase. In the second heating cycle it was observed that the T_g of the PBHS copolymers varied from −23 to −1 °C. Compared to pure PBS, the copolyesters showed a significant increase of the T_g with increasing hydantoin content. This was due to the rigidity of the hydantoin units, which caused a restricted segmental mobility and thereby an increase of the glass transition temperature. The homopolyester of H-diol with DMS (PHS) showed no melting peak and copolyesters with high amounts of HS units were also amorphous; only the polyester with 10 mol% of HS units comprised crystallinity.

The aforementioned results indicated a significant influence of the rigid hydantoin units on the crystallization tendency of PBS. Therefore, it was also important to determine the spherulitic structure of the copolyesters in order to illustrate the relationship between chemical composition and crystallization behavior of the copolyesters. In this study, the spherulitic structure and morphology of PBS and the copolyesters were studied by WAXD and POM, respectively. Figure 4 shows the WAXD patterns of PBS and the copolyesters; it could be observed that $PB_{90}H_{10}S$ and $PB_{80}H_{20}S$ exhibited two major reflexes at $2\theta = 19.8$ and 22.7°, just as PBS. This proved the similarity regarding the spherulitic structure among copolyesters with HS units and PBS. The incorporation of low amounts, i.e. up to 20 mol%, did not disturb the PBS spherulitic structure to a large extent. Furthermore, the spherulitic morphology of PBS and the copolyesters was investigated by POM, as depicted in Figure 4. In pure PBS, the spherulites exhibited a well-defined fibrillar pattern with an apparent Maltese cross.[26] Incorporation of an increasing amount HS units in the copolyester backbone led to a change in the spherulitic morphology along with a smaller diameter. This effect was even more significant in copolyesters with more than 20 mol% HS units, which can be attributed to the reduced crystallization ability after incorporation of HS units.

Table 3. Melt polycondensation of DMS, BDO, and H-diol: thermal properties of the copolyesters.

Sample	T_g [°C]	T_m [°C]	ΔH_m [J g^{-1}]	T_c [°C]	ΔH_c [J g^{-1}]	T_d [°C]
PBS	−37	114	64.0	79	70	266
$PB_{90}H_{10}S$	−23	102	46.7	59	51	304
$PB_{80}H_{20}S$	−20	86	6.1	–	–	298
$PB_{70}H_{30}S$	−13	–	–	–	–	293
$PB_{60}H_{40}S$	−6	–	–	–	–	283
PHS	−1	–	–	–	–	232

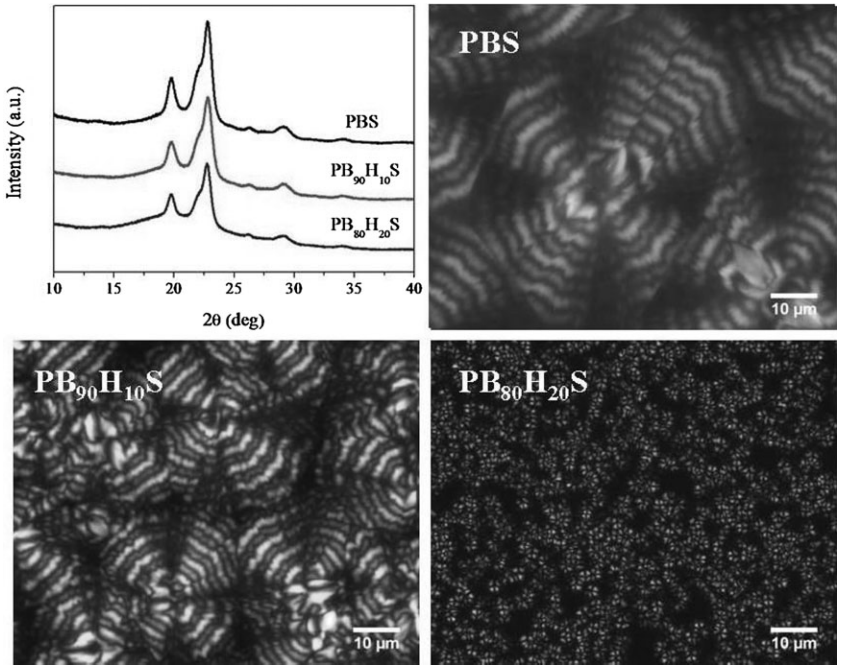

Figure 4. X-ray patterns and POM graphs of PBS and PBHS copolyesters.

3.3. Cytotoxicty of the Copolyesters

For judging the potential of new materials in biomaterial applications, the evaluation of biocompatibility is of utmost significance. Therefore, cytotoxicity of the resulting polyesters was tested using L929 cells as shown in Figure 5 and poly(ethyleneimine) 25 kDa (PEI 25 kDa) was used as the positive control for MTT assay. Irrespective of the polyester composition, all homo- and copolyesters were less-toxic than PEI 25 KDa and showed high cell viabilities. Cytotoxicity experiments using similar procedure could not be performed after chlorination since the polymers were no more soluble in water miscible solvents like acetone and THF. Therefore, a modified procedure using a chloroform solution of polymers was utilized to assess cytotoxicity by fluorimetric metabolic assay employing NIH/3T3 embryonic fibroblast cells. (details are given in Supporting Information). A stock solution of polymers in chloroform ($100\,mg \cdot mL^{-1}$) was diluted to different concentrations in the range from 2.5 to $1.19 \times 10^{-6}\,mg \cdot mL^{-1}$ using aqueous growth medium. The toxicity of chloroform was additionally measured to test its possible contribution to the toxicity derived by the copolyesters (see Supporting Information for a detailed description of the influence of the solvent on the cytotoxicity; Figure S3 and S4). Chloroform was not toxic to NIH/3T3 embryonic fibroblasts used for cytotoxicity experiments till about 1.6 vol% and therefore had no negative influence on the cytotoxicity of polymers. The IC_{50} values in order of decreasing toxicity were: PEI 25 kDa ($0.014\,mg \cdot mL^{-1}$), PB60H40S-Cl (chlorinated copolyester $IC_{50} = 0.62\,mg \cdot mL^{-1}$), PB60H40S (non-chlorinated copolyester $IC_{50} = 0.64\,mg \cdot mL^{-1}$), and PCL ($IC_{50} = 1.09\,mg \cdot mL^{-1}$) (Figure S5, Supporting Information). There was no significant difference in the IC_{50} values before and after chlorination. Also, the results clearly showed significantly reduced toxicity of the polymers made in this work in comparison to PEI, a well established bio polymer. The polymers before or after chlorination were at least 100 times less toxic than PEI.

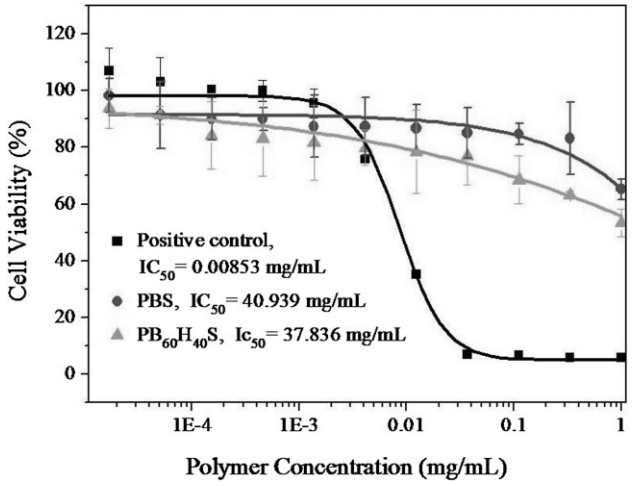

Figure 5. Viability of L929 cells depending on the concentration of PBS and $PB_{60}H_{40}S$, respectively, as determined via MTT assay.

3.4. Enzymatic Degradation of Copolyester

The enzymatic degradation behavior of the copolyesters before and after chlorination was investigated using *Pseudomonas cepacia* lipase in phosphate buffer at 37 °C. Weight loss and the morphological changes of chlorinated and unchlorinated $PB_{70}H_{30}S$ copolyester films during the enzymatic degradation process are presented in Figure 6. The material was degraded completely within 12 d. Before contact to the enzyme, the film surface was smooth and did not comprise any holes; after immersion into the enzyme solution for 6 d, the film exhibited many cracks and a porous structure.

3.5. Antibacterial Properties

Antibacterial properties were measured for samples before and after chlorination. The improvement of antibacterial

Macromolecular Journals

Macromol. Biosci. **2012**, DOI: 10.1002/mabi.201100520

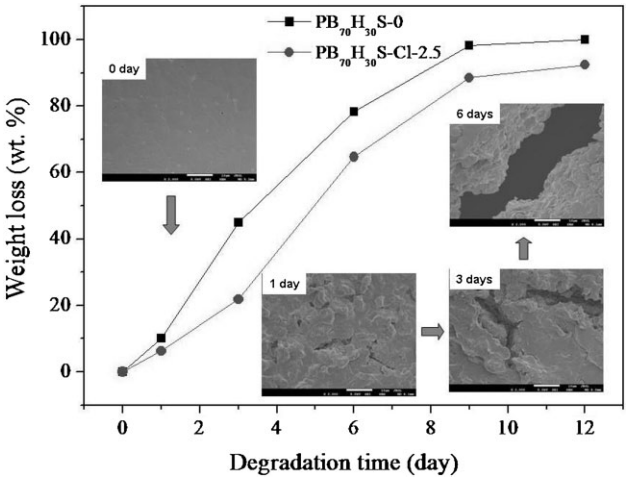

Figure 6. Weight loss versus time of $PB_{70}H_{30}S$-o and $PB_{70}H_{30}S$-2.5 copolyester films and the morphology evolution of $PB_{70}H_{30}S$-o copolyester film during enzymatic degradation.

action in the chlorinated material is obvious (see Supporting Information Figure S6). It shows the colony formation of the undiluted washing solution after spreading on nutrient agar and incubation. Both, untreated control (A) and *N*-halamine polyester (B), bleach treated for 2.5 h, had 60 min contact to the bacteria. Although untreated sample also showed antibacterial action but it can be seen, that a total reduction took place in case of the chlorinated copolyester (see also Table 2). Table depicts the reduction of viable cells in log stages, calculated from the number of viable cells in the washing solution as determined by the spread plate method regarding the theoretical amount derived from the initial inoculum. It is obvious that a chlorination time of 2.5 h leads to a material which results in a reduction of 100% after 60 min contact to the bacteria cells.

4. Conclusion

We present an efficient method for the preparation of antibacterial polyesters with pendent *N*-halamine moieties comprising moderate molecular weights. Structural characterization of the polyesters with hydantoin functionalities was accomplished using FT-IR and NMR, respectively. The copolyesters exhibited better thermal stabilities than PBS at a lower degree of crystallinity. All copolyesters were less toxic than PEI and showed very high cell viabilities. The *N*-halamine form with a high amount of oxidative chlorine comprises an antimicrobial activity regarding *E. coli*. Hence, those copolyesters synthesized via a melt transerification possess a considerable potential for application in medical devices, hygienic materials, and the food-processing industry as antibacterial additives.

Acknowledgements: The Philipps-University Marburg is acknowledged for the financial support.

Received: December 21, 2011; Revised: January 19, 2012; Published online: DOI: 10.1002/mabi.201100520

Keywords: antibacterial; hydantoin; melt polycondensation; *N*-halamine

[1] L. H. Stoodley, J. W. Costerton, P. Stoodley, *Nat. Rev. Microbiol.* **2004**, *2*, 95.
[2] A. M. Klibanov, *J. Mater. Chem.* **2007**, *17*, 2479.
[3] O. Bouloussa, F. Rondelez, V. Semetey, *Chem. Commun.* **2008**, *8*, 951.
[4] C. J. Waschinski, J. Zimmermann, U. Salz, R. Hutzler, G. Sadowski, J. C. Tiller, *Adv. Mater.* **2008**, *20*, 104.
[5] T. Eren, A. Som, J. R. Rennie, J. F. Nelson, Y. Urgina, K. Nüsslein, E. B. Coughlin, G. N. Tew, *Macromol. Chem. Phys.* **2008**, *209*, 516.
[6] E. R. Kenawy, F. I. Abdel-Hay, A. E. R. El-Shanshoury, M. H. El-Newehy, *J. Polym. Sci., Part A: Polym. Chem.* **2002**, *40*, 2384.
[7] E. R. Kenawy, Y. A. G. Mahmoud, *Macromol. Biosci.* **2003**, *3*, 107.
[8] S. Takano, H. Tamegai, T. Itoh, S. Ogata, H. Fujimori, S. Ogawa, T. Iida, Y. Wakatsuki, *React. Funct. Polym.* **2011**, *71*, 195.
[9] I. Perelshtein, G. Applerot, N. Perkas, E. Wehrschetz-Sigl, A. Hasmann, G. M. Guebitz, A. Gedanken, *ACS Appl. Mater. Interfaces* **2009**, *1*, 361.
[10] U. Makal, L. Wood, D. E. Ohman, K. J. Wynne, *Biomaterials* **2006**, *27*, 1316.
[11] S. J. Grunzinger, P. Kurt, K. M. Brunson, L. Wood, D. E. Ohman, K. J. Wynne, *Polymer* **2007**, *48*, 4653.
[12] H. B. Kocer, A. Akdag, X. Ren, R. M. Broughton, S. D. Worley, T. S. Huang, *Ind. Eng. Chem. Res.* **2008**, *47*, 7558.
[13] J. Luo, Z. Chen, Y. Sun, *J. Biomed. Mater. Res.* **2006**, *77*, 823.
[14] X. Sun, L. Zhang, Z. Cao, Y. Deng, L. Liu, H. Fong, Y. Sun, *ACS Appl. Mater. Interfaces* **2010**, *2*, 952.
[15] Z. Chen, Y. Sun, *Ind. Eng. Chem. Res.* **2006**, *45*, 2634.
[16] M. R. Badrossamay, G. Sun, *J. Biomed. Mater. Res., Part B: Appl. Biomater.* **2009**, *89*, 93.
[17] M. R. Badrossamay, G. Sun, *Macromolecules* **2009**, *42*, 1948.
[18] Y. Sun, G. Sun, *Macromolecules* **2002**, *35*, 8909.
[19] Y. Sun, G. Sun, *J. Appl. Polym. Sci.* **2003**, *88*, 1032.
[20] Y. Sun, G. Sun, *J. Polym. Sci., Part A: Polym. Chem.* **2001**, *39*, 3348.
[21] K. Barnes, J. Liang, R. Wu, S. D. Worley, J. Lee, R. M. Broughton, T. S. Huang, *Biomaterials* **2006**, *27*, 4825.
[22] Y. Sun, G. Sun, *J. Appl. Polym. Sci.* **2001**, *80*, 2460.
[23] a) E. R. Kenawy, S. D. Worley, R. Broughton, *Biomacromolecules* **2007**, *8*, 1359; b) H. B. Kocer, I. Cerkez, S. D. Worley, R. M. Broughton, T. S. Huang, *ACS Appl. Mater. Interfaces* **2011**, *3*, 3189; c) I. Cerkez, H. B. Kocer, S. D. Worley, R. M. Broughton, T. S. Huang, *Langmuir* **2011**, *27*, 4091; d) H. B. Kocer, S. D. Worley, R. M. Broughton, T. S. Huang, *React. Funct. Polym.* **2011**, *71*, 561.
[24] X. Wei, Z. Wang, J. Chen, J. Wang, S. Wang, *J. Membr. Sci.* **2010**, *346*, 273.
[25] S. D. Worley, F. Li, R. Wu, J. Kim, C. I. Wei, J. F. Williams, J. R. Owens, J. D. Wander, A. M. Bargmeyer, M. E. Shirtliff, *Surf. Coat. Int., Part B: Coat. Trans.* **2003**, *86*, 273.
[26] W. Zhou, S. Yuan, Y. Chen, L. Bao, *J. Appl. Polym. Sci.* **2012**, *124*, 3124.